



A New Class of Oxyimides: Oxyimide Ethers and their Use as Flame Retardants

Bianca Spieß, Elke Metzsch-Zilligen, and Rudolf Pfaendner*

Oxyimides have gained wide interest in different applications because of radical generating properties, such as flame retardants in various polymers. As polyamide-6 (PA6) is highly flammable and shows burning dripping during incineration the mentioned issues have to be overcome by the use of a flame retardant. All previously developed oxyimides already show these properties, but this is based on the ester structure with the consequence of transesterification/transamidation in polyesters/polyamides. In this work, a new class of oxyimides based on ether bonds is synthesized. Oxyimide ethers do not degrade PA6, only sometimes slightly increase MVR, and show excellent flame retardancy in PA6. Depending on the structure, UL 94 V-0 can be reached with very low loadings. This makes oxyimide ethers an alternative to commonly used flame retardants for PA6.

1. Introduction

Oxyimides have gained wide interest in different applications. They have been studied as organocatalysts for Michael addition.^[1] Kumar et al. even propose some transition state based on the oxyimide structure which is the basis for functioning as a catalyst.^[2] Furthermore oxyimides are a promoter for synthesis of porous cellulose.^[3] Based on its radical generating nature oxyimides are also used as oxygen scavenger in polypropylene (PP).^[4] Moreover they are a source of oxygen scavengers in a component of fluoroimide based plant disease control agents.^[5] As radicals are known to degrade polymers^[6,7] and influence heat release, ignition and flammability^[8] radical generators can be employed as flame retardants for various polymers.^[9] Therefore, oxyimides were applied in different formulations as flame retardants especially in PP.^[10,11] In this work a new class of oxyimides based on the oxyimide ether-structure -NOCH₂- is synthesized and investigated in polyamide 6 (PA6).

PA6 is a major technical polymer in engineering and is commercially used for different applications such as mobility,^[12] E&E,

packaging, medicine, construction, and living.^[13] Its importance is due to its properties like durability, good chemical resistance, exceptional mechanical properties and low cost raw materials.^[13,14] Because of its carbon rich backbone and the high fuel/monomer molar mass ratio PA6 is highly flammable with a major drawback of melt dripping. As chain scission is favored in PA6 ignition leads to a large flame spread and, therefore, it needs addition of flame retardants in case of fire protection is requested.^[15] Commonly utilized flame retardants, if halogen and phosphor free like melamine cyanurate, have to be incorporated in high loadings.^[16] Unfortunately, these high loadings result in a deterioration of mechanical properties. Especially injection molding can become difficult for smaller molded parts.^[17] As trends in industry involve miniaturization and higher processing productivity^[18] such impacts are objects of recent investigation.

Radical generators are known to provide flame retardancy at low concentrations through a fast and controlled degradation mechanism resulting in non-burning dripping of polymers such as polypropylene or TPU.^[6,19] Similarly melamine cyanurate induces fast degradation of unreinforced PA6 as well as non-burning dripping.^[20] Therefore, the investigation of oxyimides as representative radical generators on flame retardancy of PA6 is a potential way to develop formulations with low loadings. However, the known oxyimides are mainly based on ester structures and may inherently cause transesterification/transamidation reactions with PA6.^[11] In order to overcome these issues corresponding oxyimide ethers are synthesized for the first time. Additionally, a synergistic effect between C-N-groups and benzene rings was proposed for flame retardants in PA6 shown with Schiff base containing polysiloxanes.^[21] Thus, this work focusses on oxyimide ethers with aromatic residues.

2. Experimental Section

All chemicals were purchased at VWR (Darmstadt, Germany) and applied without further purification or drying steps. PA6 was provided by Lanxess AG (Köln, Germany) and belongs to the Durethan B 30 S product line. PA6 was milled with a Retsch SM200 (Retsch GmbH, Haan, Germany) and dried prior to extrusion. ¹H-NMR was carried out in a Bruker Nanobay 300 spectrometer (Bruker GmbH, Mannheim, Germany) in DMSO-d₆ or HFIP-d₁ at 300 MHz and ¹³C-NMR in the same spectrometer and solvent at 76 MHz. Spectra were analyzed via MestReNova. For TGA measurements a TGA/DSC 1 Star system

B. Spieß, Dr. E. Metzsch-Zilligen, Prof. R. Pfaendner
Fraunhofer Institute for Structural Durability and System Reliability LBF
Schlossgartenstr. 6, Darmstadt 64289, Germany
E-mail: rudolf.pfaendner@lbf.fraunhofer.de

The ORCID identification number(s) for the author(s) of this article can be found under <https://doi.org/10.1002/mame.202000650>.

© 2021 The Authors. Macromolecular Materials and Engineering published by Wiley-VCH GmbH. This is an open access article under the terms of the Creative Commons Attribution-NonCommercial-NoDerivs License, which permits use and distribution in any medium, provided the original work is properly cited, the use is non-commercial and no modifications or adaptations are made.

DOI: 10.1002/mame.202000650



of Mettler Toledo (Giessen, Germany) was used and DSC was measured with a DSC822 of Mettler Toledo (Giessen, Germany). Both graphs were studied with STARe Evaluation Software. Melting points were determined via Melting Point M-560 made by Büchi (Essen, Germany). Compounds were extruded on a Thermo Fisher Process11 (Thermo Scientific GmbH, Dreieich, Germany), a twin screw extruder for small scale extrusions operated at a screw speed of 150 rpm, feeder speed of 10 rpm, temperature of 230 °C and under vacuum and with under-water strand granulation. The granulate was injection molded after drying at 80 °C by a Babyplast 6/10P (Christmann Kunststofftechnik GmbH, Kierspe, Germany) at 280 °C, injection speed of 90%, pressure of 60 bar and cooling time of 1.2 s into UL 94 test bars of size 127 mm x 13.5 mm x 3.2 mm (*L* x *B* x *H*). Melt volume flow rate (MVR) was taken according to DIN EN ISO1133 with a MI2 made by Göttfert (Buchen, Germany) at 250 °C and 2.16 kg with 6.0 g and a melting time of three minutes. Burning behavior was examined via UL94 and ISO 1210 in an UL94 chamber of Wazau (Berlin, Germany) and additionally by an infrared camera PI400 made by Opiris (Berlin, Germany).

2.1. General Synthetic Procedure

α,α'-Bis(phthalimide-N-oxy)-xylene (*o*PIBE(1), *m*PIBE(2),^[23] *p*PIBE(3)):

2.93 g (0.011 mol, 1 eq) *α,α'*-dibromo-xylene and 3.68 g (0.022 mol, 2 eq) *N*-hydroxyphthalimide are dissolved in 60 mL acetonitrile while flushing with nitrogen. After stirring under reflux for 30 min 3.5 mL (0.025 mol, 2 eq) triethylamine is added. The mixture is stirred under reflux for four more hours and at room temperature for 1.5 days. The product is filtrated, washed with ice-cold acetonitrile and precipitated with methanol for purification.

α,α''-Bis(naphthalimide-N-oxy)-xylene (*o*NIBE(4), *m*NIBE(5), *p*NIBE(6)):

2.40 g (0.005 mol, 1 eq) *α,α'*-dibromo-xylene and 1.48 g (0.011 mol, 2 eq) *N*-hydroxynaphthalimide are dissolved in 50 mL acetonitrile while flushing with nitrogen. After stirring under reflux for 30 min 3.0 mL (0.021 mol, 4 eq) triethylamine is added. The mixture is stirred under reflux for four more hours and at room temperature for 1.5 days. The product is filtrated, washed with ice-cold acetonitrile and purified by adding

methanol to the crude solid, stirring at room temperature for four hours, filtrating and washing the crystals with additional methanol.

1,3,5-tris(benzylxyloxy)-1,3,5-triazinane-2,4,6-trione (TBCU(7)):^[24]

2.14 g (0.01 mol, 1 eq) diphenylcarbonate are finely grounded with a pestle and mixed with 1.60 g (0.01 mol, 1 eq) *O*-benzylhydroxylamine hydrochloride and 2.44 g (0.02 mol, 2 eq) 4-dimethylamino pyridine. The mixture is heated under nitrogen at 120 °C for one hour. After cooling to room temperature, 30 mL methanol is added and the mixture is stirred at room temperature for three hours. The product is filtrated and washed with methanol for purification.

The synthesized oxyimide ethers were characterized through ¹H-NMR, TGA, and melting point apparatus (Table 1).

All materials showed high purity without any detectable by-products, representative spectra is shown as Figure 1:

The NMR displays no signal between 9.0 and 12.0 ppm where the OH-signal of persistent educt would appear. This shows there is also no educt left in the purified product and manufacturing was successful.

As solubility of oxyimide ethers except TBCU in common NMR solvents (acetone-d₆, acetonitrile-d₃, CDCl₃, DMF-d₇, DMSO-d₆, ethanol-d₆, pyridine-d₅, THF-d₈, toluene-d₈, D₂O) is very small, a ¹³C-NMR-analysis in DMSO is only possible for TBCU. Representative the ¹³C-NMR of TBCU is shown in Figure 2:

NMR spectra of the other oxyimide ethers are taken in deuterated trifluoro acetic acid and can be found in the supporting information.

3. Results and Discussion

3.1. Synthesis and Characterization

Oxyimides have been synthesized mainly via Williamson ether synthesis.^[2,22] Seven different *bi*- and *trifunctional* oxyimide ethers have been produced via Williamson ether synthesis in a modified way according to Bell et al.^[23] or via amid-ether-synthesis as stated by Hirai et al.^[24] All have aromatic residues and all except one possess an aromatic basis, too. For aromatic basis *ortho*, *meta*, or *para* substituted benzene has been chosen in order to get possible synergism between nitrogen and benzene or pi-stacking. This leads to the following seven oxyimide ethers:

Table 1. Characterization of oxyimide ethers.

oxyimide	T _{dec} ^{2%} [°C]	T _{dec} ^{5%} [°C]	T _{dec} ^{10%} [°C]	T _m [°C]	color	¹ H-NMR (DMSO-d ₆ , 300 MHz, δ)
<i>o</i> PIBE (1)	275	283	288	277	Pink	7.9 (d, <i>J</i> = 1.5 Hz, 8H, CH); 7.6 (m, 2H, CH); 7.4 (dd, <i>J</i> = 5.6 Hz, 3.4 Hz, 2H, CH); 5.5 (s, 4H, CH ₂)
<i>m</i> PIBE (2)	278	288	295	230	Pink-white	7.9 (s, 8H, CH); 7.7 (d, <i>J</i> = 1.8 Hz, 1H, CH); 7.6 (m, 2H, CH); 7.5 (dd, <i>J</i> = 8.5 Hz, 6.5 Hz, 1H, CH); 5.2 (s, 4H, CH ₂)
<i>m</i> PIBE lit. ^[23]	n.d.	n.d.	n.d.	222	white	7.82-7.71 (m, 8H, phthal-ArH), 7.67 (s, 1H, ArH), 7.59 (dd, <i>J</i> = 8 Hz, 1 Hz, 2H, ArH), 7.43 (t, <i>J</i> = 8 Hz, 1H, ArH), 5.21 (s, 4H, ArCH ₂)
<i>p</i> PIBE (3)	221	263	293	304	colorless	7.9 (s, 8H, CH); 7.6 (s, 4H, CH); 5.2 (s, 4H, CH ₂)
<i>o</i> NIBE (4) ^{a)}	230	251	270	268	Off-white	8.9 (m, 2H, CH); 8.6 (m, 8H, CH); 8.0 (m, 4H, CH), 7.9 (dd, <i>J</i> = 5.7 Hz, 3.4 Hz, 2H, CH)
<i>m</i> NIBE (5) ^{a)}	226	242	256	283	pink	8.5 (m, 8H, CH); 7.9 (dd, <i>J</i> = 8.4 Hz, 7.3 Hz, 4H, CH); 5.3 (s, 4H, CH)
<i>p</i> NIBE (6) ^{a)}	243	292	314	299	Colorless	8.5 (m, 8H, CH); 7.9 (q, <i>J</i> = 8.6 Hz, 8.6 Hz, 8.0 Hz, 4H, CH); 5.3 (d, <i>J</i> = 8.2 Hz, 4H, CH)
TBCU (7)	229	246	257	238	colorless	7.5 (dt, <i>J</i> = 29.1 Hz, 5.3 Hz, 4.8 Hz, 3.0 Hz, 15H, CH); 5.1 (s, 6H, CH ₂)

^{a)}shows only slight solubility in DMSO.

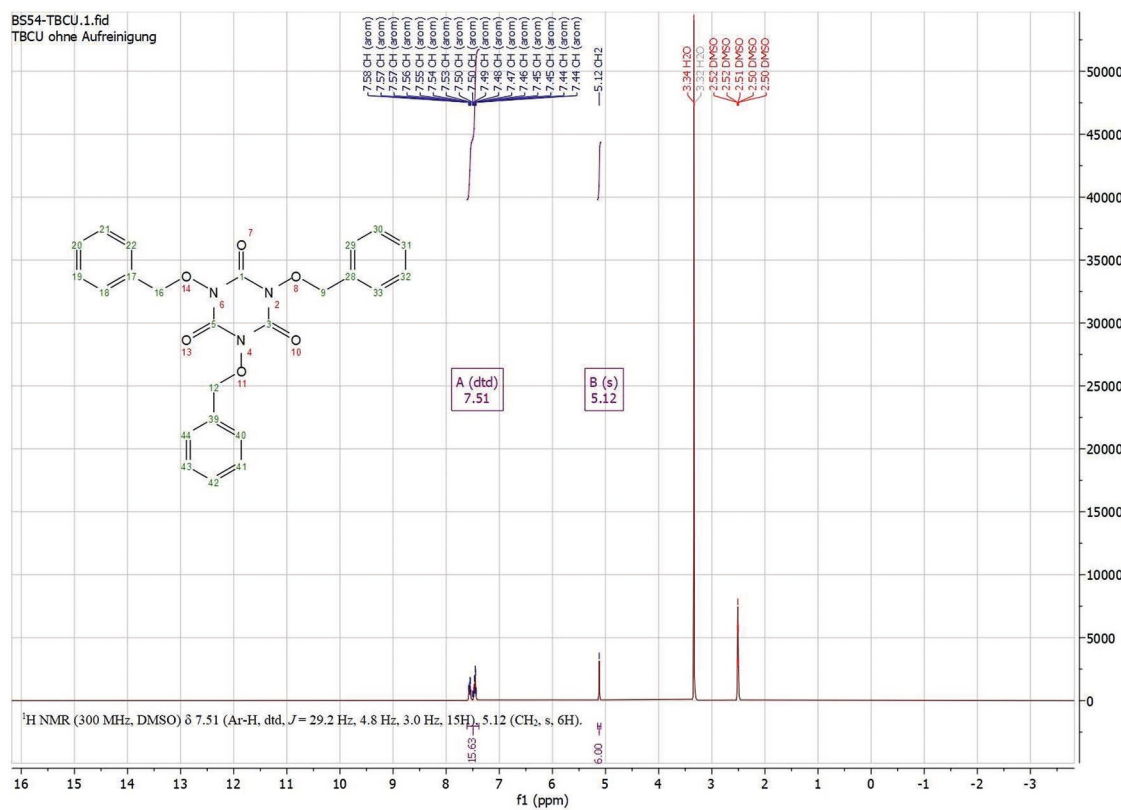


Figure 1. ¹H-NMR TBCU (300 MHz, DMSO-d₆, δ): 5.1 ppm (s, 6H, CH₂); 7.5 ppm (dtd, 15H, Ar H).

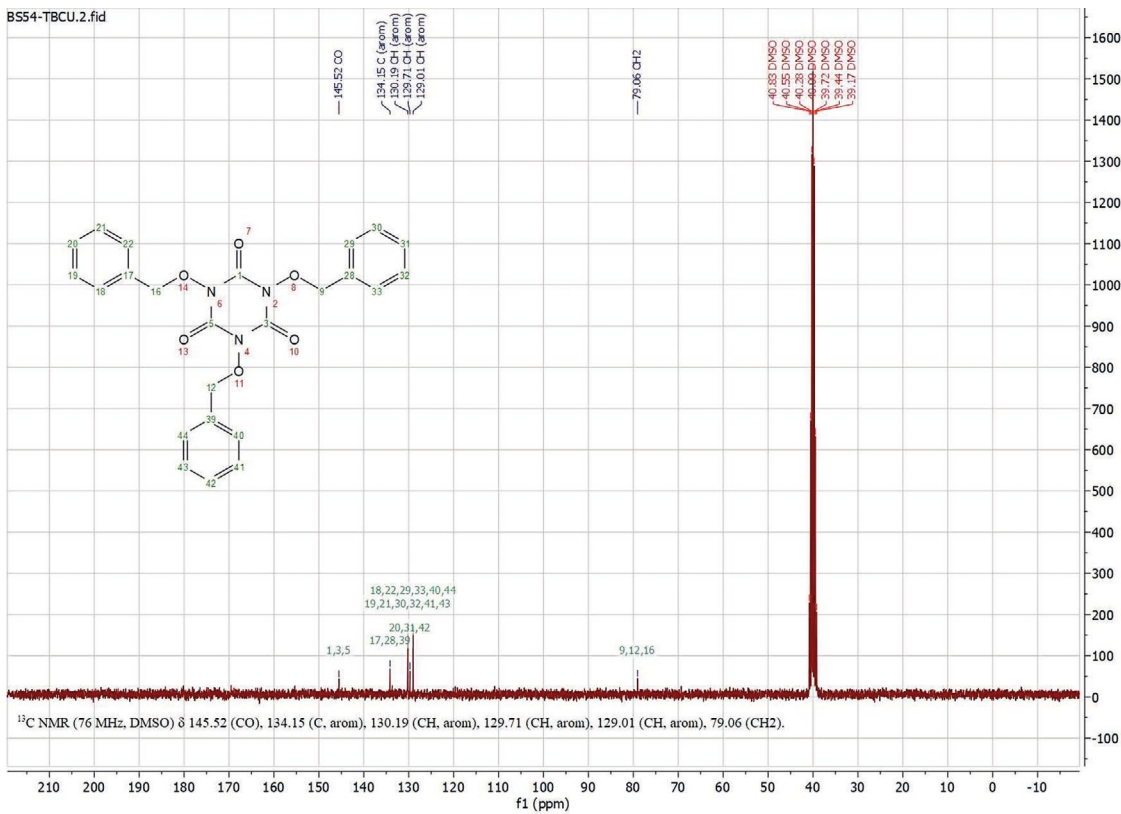
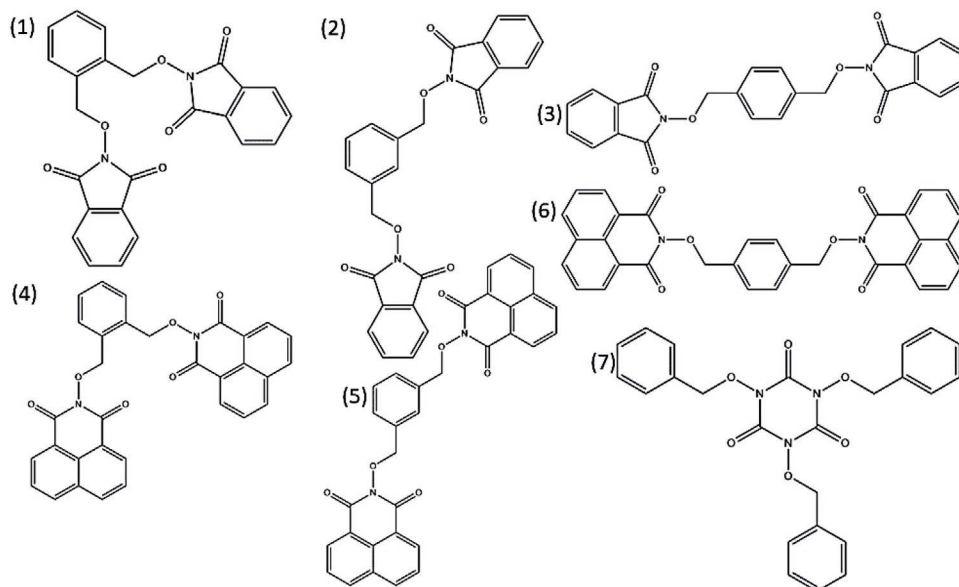


Figure 2. ¹³C-NMR of TBCU (76 MHz, DMSO-d₆, δ): 145.5 (s, C4); 134.2 (s, C4); 130.2 (s, CH); 129.7 (s, CH); 129.0 (s, CH); 79.0 (s, CH₂).



1. 2,2'-(1,2-phenylenebis(methylene))bis(oxy)bis(isoindoline-1,3-dione) (oPIBE)
2. 2,2'-(1,3-phenylenebis(methylene))bis(oxy)bis(isoindoline-1,3-dione) (mPIBE)
3. 2,2'-(1,4-phenylenebis(methylene))bis(oxy)bis(isoindoline-1,3-dione) (pPIBE)
4. 2,2'-(1,2-phenylenebis(methylene))bis(oxy)bis(1H-benzo[de]isoquinoline-1,3(2H)-dione) (oNIBE)
5. 2,2'-(1,3-phenylenebis(methylene))bis(oxy)bis(1H-benzo[de]isoquinoline-1,3(2H)-dione) (mNIBE)
6. 2,2'-(1,4-phenylenebis(methylene))bis(oxy)bis(1H-benzo[de]isoquinoline-1,3(2H)-dione) (pNIBE)
7. 1,3,5-tris(benzylxoxy)-1,3,5-triazinane-2,4,6-trione (TBCU)

Oxyimide ether (1) – (3) are all based on phthalimide whereas (4) – (6) are compiled on naphthalimide. Oxyimide ether (7) in contrast is made by a ring-closure reaction, the amid-ether-synthesis.^[24] This reaction cannot be carried out in solution but has to be a solid phase reaction in order to get the fully connected ring; in a solution, the six molecules for full ring closure statistically do not stay long enough nearby to react.

3.2. Thermal Stability

The synthesized oxyimide ethers are thermally stable up to 270 °C the lowest and 313 °C the highest. Comparing the TGA's of the ones with the same chemical basis para-substituted oxyimide ethers are the most stable ones (Figure 3).

In the case of a phthalimide basis, the *ortho*-substituted oxyimide ether is slightly less stable than the *meta*-substituted one. In case of a larger ring system the *meta*-substituted oxyimide ether is less stable. *m*NIBE excluded, the oxyimide ethers based on naphthalimide show higher degradation temperatures than the ones based on phthalimide. This is due to a lower sterical energy calculated with Chem3D. In contrast to the PIBE series, the NIBE sequence has negative energies and is consequently more resistant against external energy supply by heat. Comparing degradation temperatures of all synthesized oxyimides a trend is obvious: Increasing content of aromatic moieties leads to higher temperature stability. This can be understood in terms of pi-stacking as those intermolecular interactions lead to a higher stability. Nevertheless

all shown new flame retardants are suitable for extrusion in PA6 at 230 °C.

3.3. Processing

In order to investigate the potential flame retardancy contribution of the oxyimide ethers in PA6 compounding and injection molding is performed whereas loadings of 1%, 2%, and 3% were used. The presented synthesized flame retardants were mostly incorporated with insignificant degradation of the polymer matrix. Furthermore, MVR-measurements give an indicator how much degradation takes place throughout the process (Table 2).

At 1% concentration none of the oxyimide ethers displays significant increase in MVR. Only *o*PIBE shows a slight growth of $20 \text{ cm}^3 10 \text{ min}^{-1}$ which is more likely to be because of oxyimide – metal interaction. Woods and King III showed that interactions between hydrogen bonds and a small hydride layer on the surface of metal parts cause a lowering of melt pressure.^[25] The same mechanism leads to higher MVR in oxyimide ether compounds. The increase of MVR when comparing 1% with 2% or 3% concentration in *m*PIBE is due to a lubricating effect as a higher loading enlarges the free volume between the polymer chains facilitating polymer chain motion,^[26] which is in line with the description of Amintowlieh et al. as the melting temperature of the compounds is not effected by incorporation of oxyimide ethers (Supporting information) but MVR is increased. The higher MVR compared to pure PA6 is not

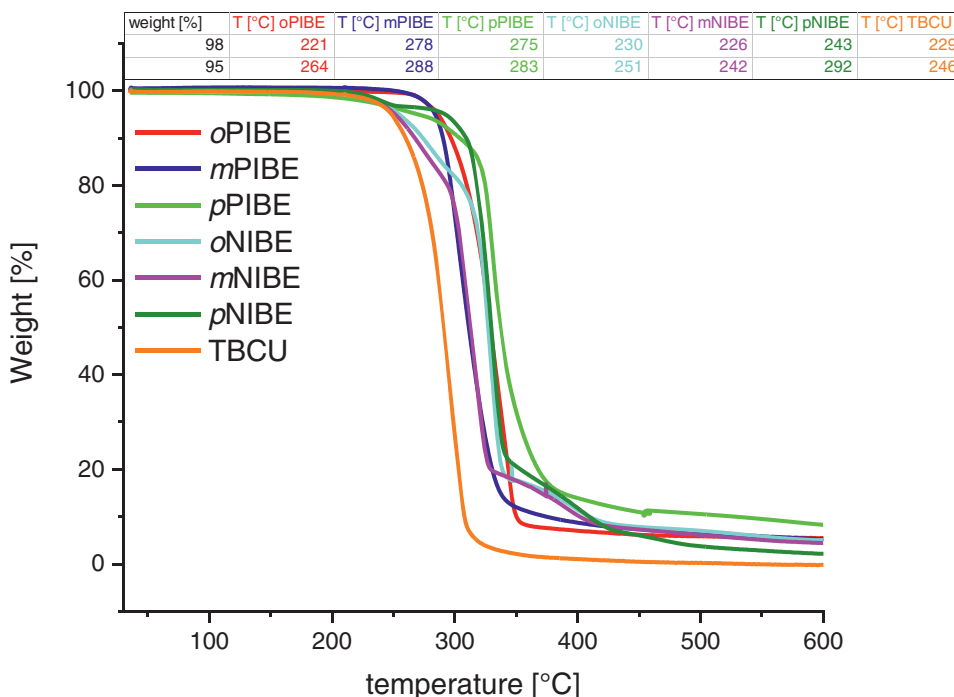


Figure 3. TGAs of *o*PIBE (red), *m*PIBE (blue), *p*PIBE (green), *o*NIBE (cyan), *m*NIBE (magenta), *p*NIBE (olive), and TBCU (orange) showing the thermal stability of those oxyimide ethers in comparison.

Table 2. MVR in $\text{cm}^3 \text{10 min}^{-1}$ of oxyimide ethers extruded with PA6 in 1% concentration, 2% concentration, and 3% concentration. Pure PA6 shows a MVR of $44 \text{ cm}^3 \text{10 min}^{-1}$.

	TBCU	<i>o</i> PIBE	<i>m</i> PIBE	<i>p</i> PIBE	<i>o</i> NIBE	<i>m</i> NIBE	<i>p</i> NIBE
MVR at 1%	34	61	46	47	48	43	38
MVR at 2%	41	109	83	75	111	63	51
MVR at 3%	51	136	100	110	173	106	53

necessarily a bad result as a lower viscosity can lead to shorter residence time in extruder or injection molding.^[26] Besides, with reduced viscosity polymers can be injection molded in

smaller parts more easily.^[27] Technically an increase of MVR can be a hint of degradation of the polymer but GPC evaluation of extruded granules did not show any significant degradation (Figure 4).

In comparison *o*NIBE does not change GPC results of pure PA6 at all and TBCU and *p*PIBE lead to a slight shift of -5.743 kDa (*p*PIBE) and $+6.331 \text{ kDa}$ (TBCU). If oxyimide ethers degrade PA6 during processing a significant shift to smaller molecular mass would be obvious in GPC.

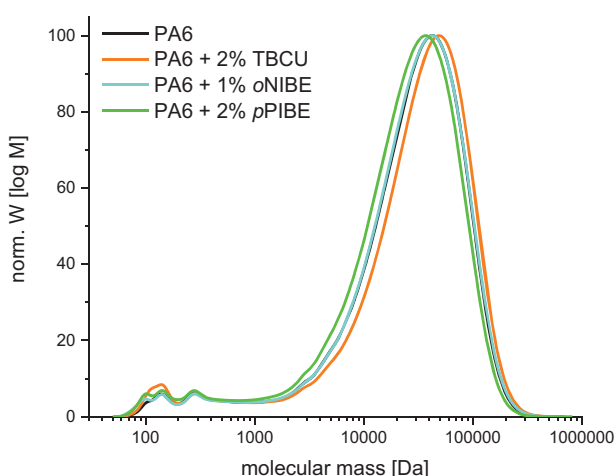


Figure 4. GPC measurement of pure PA6 and some oxyimide ether compounds.

3.4. Flame Retardancy

UL94 test is a general procedure to explore burning behavior and flame resistance of polymers resulting in three categories. The lowest category is V-2 meaning the sample is flammable, self-extinguishing and spreads fire by burning drops. V-1 has no burning drops and V-0 extinguishes even faster than V-1. Non-extinguishing samples cannot be classified. All formulations are tested with five specimens (Table 3).

The addition of oxyimide ethers improves the flame resistance of PA6 independently of the structure. Pure PA6 gives five records V-2 with a total burning time of 38.3 s. due to multiple



Table 3. UL94 results of oxyimide ethers extruded in 1% concentration, 2% concentration, and 3% concentration. Pure PA6 gives five times V-2 taking a total burning time of 38.3 s.

	TBCU	<i>o</i> PIBE	<i>m</i> PIBE	<i>p</i> PIBE	<i>o</i> NIBE	<i>m</i> NIBE	<i>p</i> NIBE
UL94 result with 1% flame retardant	5xV-2	5xV-2	5xV-2	5xV-2	1xV-0 4xV-2	5xV-2	5xV-2
burning time	27.7 s	12.4 s	15.0 s	6.1 s	19.0 s	19.0 s	12.7 s
UL94 result with 2% flame retardant	3xV-0 2xV-2	1xV-0 4xV-2	5xV-2	4xV-0 1xV-2	2xV-0 3xV-2	1xV-0 4xV-2	2xV-0 3xV-3
burning time	8.9 s	7.2 s	14.3 s	0.0 s	3.0 s	9.3 s	7.9 s
UL94 result with 3% flame retardant	1xV-0 4xV-2	3xV-0 2xV-2	5xV-2	3xV-0 2xV-2	4xV-0 1xV-2	5xV-2	5xV-2
burning time	12.6 s	1.3 s	23.6 s	3.5 s	2.0 s	7.9 s	13.9 s

burning drips of the polymer resulting in a burning mass of drained PA6. Best outcome of the tested samples results with 2% *p*PIBE or 3% *o*NIBE in four out of five times V-0. Increasing the concentration of *o*PIBE or *m*PIBE to 5% shows five times V-0. Adding oxyimide ether lowers the amount of burning drips. Most occurring droplets are non-burning. The remaining V-2 of one sample is because of one burning polymer drip igniting the cotton wool. A worse UL94 result with higher concentration is due to too large drips taking heat and the flame down to the cotton wool. Infrared videos of the scorching process show the surface temperature of flame-retarded specimens is about ten degrees lower than the one of pure PA6. This cooling effect can be used to suppress burning droplets. Still with 2% *p*PIBE one sample is not cooled enough to give UL94 V-0. Additionally the outside touched by the flame expresses some surface effect. No intumescence or charring but a glassy layer occurs (**Figure 5**):

The left part clearly reveals the above mentioned glassy layer. Thickness does not vary significantly. SEM pictures confirm a smooth top within the burned area whereas the non-burned district, which is only heated by hot air, displays a rough surface in accordance to commonly seen surface roughness of PA6.^[28] In the transition zone fewer and more round cavities occur looking like gas evolution has taken place. According to EDX the burned spot contains 3% less nitrogen and 2% less

oxygen than the non-burned region indicating the oxyimide ether gassed out and reacted in the gaseous phase (**Figure 6**).

Interestingly pure PA6 demonstrates the opposite behavior. The non-burned area is smooth, displays no holes and only has some stripes occurring along the injection molding direction. The burned zone shows small round cavities like the transition zone in the flame-retarded sample. As far as known up to date, the glassy layer only arises in PA6 flame retarded with oxyimide ethers. As they are radical generators, they are capable of degrading PA6. Degraded PA6 flows together and oxyimide ether decomposition or reaction products gassing out resulting in the glassy layer protecting the sample against the flame. Therefore, oxyimide ethers react in the condensed phase. Moreover, they can act in the gaseous phase and stopping radical reactions.

4. Conclusion

Seven different oxyimide ethers have been successfully synthesized via easily accessible routes. All are suitable for extrusion in PA6 as they show sufficient thermostability above 270 °C. MVR is somewhat increased likely through oxyimide – metal – interactions. As oxyimide ethers react in gaseous

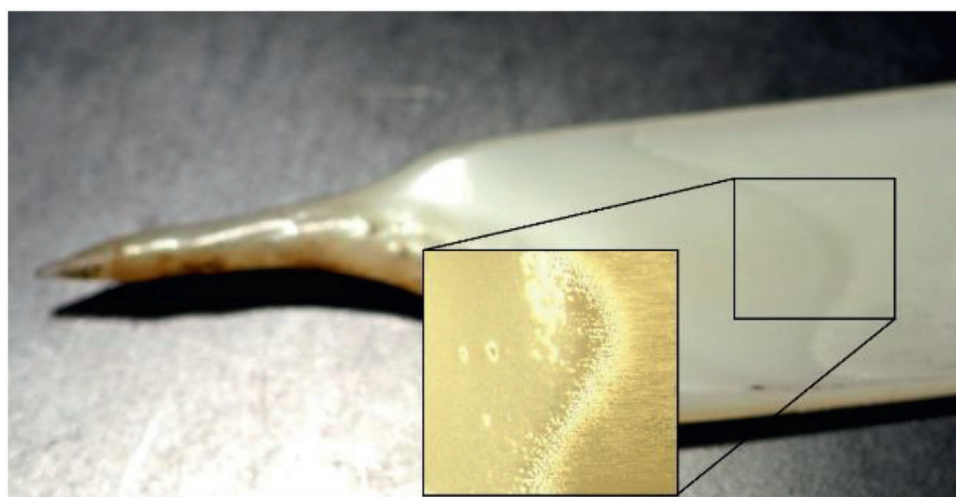


Figure 5. Microscopic picture of PA6 with 1% *m*PIBE. 10x magnification in rectangle.

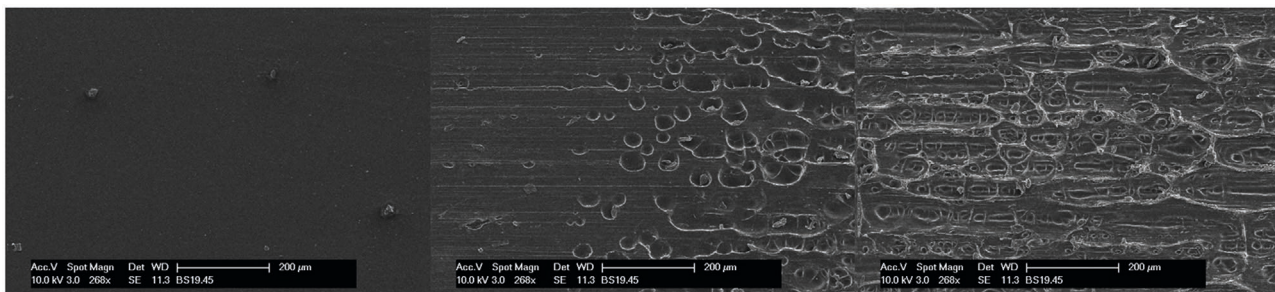


Figure 6. SEM pictures of PA6 + 2% oPIBE at 268x magnification of the burned zone (left), transition area (middle) and non-burned area (right) (additional pictures in Supporting Information).

as well as condensed phase they display excellent flame retardancy already in low concentrations. V-0 can be achieved with 2% concentration only depending on the molecule structure, which is a decisive improvement compared to commonly used melamine cyanurate which has to be incorporated in concentrations between 8% and 15%. The decreased flammability attained in the compounds is due to a combination of non-burning dripping, cooling and shielding by a glassy layer. This flame retarding mechanism is very different to commonly seen intumescence also in PA6. Usually intumescence occurs with charring and the layer can be compact on the outside, on the contrary the surface of the glassy layer of the present tests is unusually smooth. Oxyimide ethers combine the advantages of halogen-free, good flame retardancy and high efficiency.

Received: October 19, 2020

Revised: November 25, 2020

Published online:

Supporting Information

Supporting Information is available from the Wiley Online Library or from the author.

Acknowledgements

This work was supported by Songwon International AG Frauenfeld, which is gratefully acknowledged.

Open access funding enabled and organized by Projekt DEAL.

Conflict of Interest

The authors declare no conflict of interest.

Author Contributions

B.S. was involved in methodology, validation, formal analysis, investigation, writing original draft, and visualization. E.M.-Z. was involved in supervision and funding acquisition. R.P. was involved in conceptualization, writing review and Editing, supervision, and project administration.

Keywords

flame retardants, glassy layers, polyamides, radical generators, UL94

- [1] A. Maria Faísca Phillips, *Curr Org. Synth.* **2016**, *13*, 687.
- [2] T. P. Kumar, L. Radhika, K. Haribabu, V. N. Kumar, *Tetrahedron: Asymmetry* **2014**, *25*, 1555.
- [3] T. Shibata, Y. Morishita, Y. Ito, *US20170210871A1*, **2015**.
- [4] E. Menozzi, M. Sala, E. Galfre, *US20170043931A1*, **2015**.
- [5] F. H. A. Okada, *US20180084779A1*, **2016**.
- [6] R. Pfaendner, *C. R. Chim.* **2006**, *9*, 1338.
- [7] D. Wan, L. Ma, Z. Zhang, H. Xing, L. Wang, Z. Jiang, G. Zhang, T. Tang, *Polym. Degrad. Stab.* **2012**, *97*, 40.
- [8] K. Furusawa, T. Kawamura, Y. Akutsu, M. Arai, M. Tamura, *Atmos. Environ.* **1997**, *31*, 3363.
- [9] a) W. Pawelec, A. Holappa, T. Tirri, M. Aubert, H. Hoppe, R. Pfaendner, C.-E. Wilén, *Polym. Degrad. Stab.* **2014**, *110*, 447; b) M. Aubert, R. C. Nicolas, W. Pawelec, C.-E. Wilén, M. Roth, R. Pfaendner, *Polym. Adv. Technol.* **2011**, *22*, 1529.
- [10] a) M. M. R. Pfaendner, *US10370537B2*, **2015**; b) M. M. R. Pfaendner, *US10450442B2*, **2015**; c) M. M. R. Pfaendner, *US10364340B2*, **2015**.
- [11] R. Pfaendner, E. Metzsch-Zillingen, M. Stec, *US20160052927A1*, **2014**.
- [12] T. Moura, R. Krieger, M.-S. Mueller, C. Minx, A. Emde, *US20190359001A1*, **2017**.
- [13] K. Marchildon, *Macromol. React. Eng.* **2011**, *5*, 22.
- [14] M. S. Subbulakshmi, N. Kasturiya, Hansraj, P. Bajaj, A. K. Agarwal, *J. Macromol. Sci.* **2000**, *40*, 85.
- [15] R. E. Lyon, M. L. Janssens, in *Encyclopedia of Polymer Science and Technology*, 4th ed. (Eds: A. Seidel, M. Peterca, H. F. Mark), Wiley, Hoboken **2014**, pp. 1–70.
- [16] a) J. Markarian, *Plastics, Additives and Compounding* **2005**, *7*, 22; b) J. Zhang, M. Lewin, E. Pearce, M. Zammarano, J. W. Gilman, *Polym. Adv. Technol.* **2008**, *19*, 928.
- [17] Z.-Y. Wu, W. Xu, Y.-C. Liu, J.-K. Xia, Q.-X. Wu, W.-J. Xu, *J. Appl. Polym. Sci.* **2009**, *113*, 2109.
- [18] E. Schmitt, M. Clauss, *Halogen-free Polyamides and Polyesters for Electronics*, Berlin **2008**.
- [19] W. Pawelec, M. Aubert, R. Pfaendner, H. Hoppe, C.-E. Wilén, *Polym. Degrad. Stab.* **2012**, *97*, 948.
- [20] Y. Liu, Q. Wang, *J. Polym. Res.* **2009**, *16*, 583.
- [21] S. Fan, B. Peng, R. Yuan, D. Wu, X. Wang, J. Yu, F. Li, *Composites, Part B* **2020**, *183*, 107684.
- [22] A. M. Ibrahim, V. Mahadevan, M. Srinivasan, *J. Polym. Sci., Polym. Chem. Ed.* **1981**, *19*, 687.
- [23] T. W. Bell, V. J. Santora, *J. Am. Chem. Soc.* **1992**, *114*, 8300.



- [24] N. Hirai, T. Kagayama, Y. Tatsukawa, S. Sakaguchi, Y. Ishii, *Tetrahedron Lett.* **2004**, *45*, 8277.
- [25] S. S. Woods, R. E. KingIII, C. Lavallée, The Influence of Polymer Process Additives (PPAs) and Hindered Amine Light Stabilizer (HALS) Combinations in LLDPE Blown Film – Part IIA, 07th ed., USA **2001**.
- [26] Y. Amintowlieh, A. Sardashti, L. C. Simon, *Polym. Compos.* **2012**, *33*, 976.
- [27] F. Baldi, A. Bongiorno, I. Fassi, A. Franceschini, C. Pagano, T. Riccò, R. Surace, F. Tescione, *Polym. Eng. Sci.* **2014**, *54*, 512.
- [28] BASF SE, Ultramid Structure: LGF-Kunststoffe für Metall-Fans.